Key Factors Affecting the Manufacture of Hydrophobic Ultrafiltration Membranes for Surface Water Treatment

Huyen T. Dang,[1] Dipak Rana,[2] Roberto M. Narbaitz,[1] Takeshi Matsuura[2]

[1]*Department of Civil Engineering, University of Ottawa, Ottawa, Ontario, Canada K1N 6N5*
[2]*Department of Chemical and Biological Engineering, University of Ottawa, Ottawa, Ontario, Canada K1N 6N5*

Received 27 July 2009; accepted 7 November 2009
DOI 10.1002/app.31739
Published online 27 January 2010 in Wiley InterScience (www.interscience.wiley.com).

ABSTRACT: As part of the development of poly(ether sulfone) (PES) membranes whose surface is modified by the incorporation of a newly synthesized hydrophobic surface modifying macromolecule (nSMM) additive, this study investigates the impact of four key membrane preparation factors. They are concentration of PES, concentration of nSMM, casting thickness, and casting speed. The synthesis and characterizations of nSMM by nuclear magnetic resonance, gel permeation chromatography, differential scanning calorimeter, and elemental analysis have been presented. The changes in characteristics and performance of the membranes have been evaluated via Fourier transform infrared spectroscopy, contact angle analysis, scanning electron microscopy, and solute transport tests. The addition of 0.5 wt % of nSMM increased the contact angle of PES membranes by 20°; however, higher nSMM concentrations did not increase the hydrophobicity any further. Only the additive concentration had a statistically significant impact on flux reduction and dissolved organic carbon rejection. Even though other factors such as membrane thickness may alter the pore characteristics, their effect on membrane performance was marginal. © 2010 Wiley Periodicals, Inc. J Appl Polym Sci 116: 2626–2637, 2010

Key words: polymeric membranes; hydrophobic additive; key modification factors; solute rejection; mathematical model

INTRODUCTION

Porous integrally asymmetric membranes are often made by the phase inversion method.[1,2] This method is applied mainly in the preparation of membranes for dialysis, microfiltration (MF), and ultrafiltration (UF). Most commercial UF membranes are cast via this technique using a multicomponent solution containing polymer(s), solvent(s), and nonsolvent(s) or additive(s). In many cases, the pore characteristics (porosity and pore size) and skin layer morphology are modified by blending additives to the casting solution.[3] The additives can be inorganic salts (e.g., $LiNO_3$, LiCl, and $ZnCl_2$), organic polymers (e.g., poly(vinyl pyrrolidone) (PVP), poly(ethylene glycol) (PEG), sulfonated poly(ether ether ketone), methacryloyloxyethylphosphorylcholine (MPC) copolymer, and poly(amide imide) (PAI)), or nanoparticles (e.g., TiO_2 and Al_2O_3).[4–12] Although PVP or PEG acts as a surface modifying additive, their effects are temporary because they are water soluble and eventually leach out from the modified membrane. Since the 1990s, our research group has been involved in the development of different types of hydrophobic surface modifying macromolecules (SMMs) to modify the membrane surface more permanently. Earlier studies with a hydrophobic SMM incorporation[13–15] did not result in a significant impact on membrane performance for drinking water treatment probably because of insufficiently migration of the particular SMM additive. A more rapidly migrating SMM has been developed (called as nSMM) for the preparation of pervaporation membranes.[16] The lead author's doctoral research plan included a comparison of the impact of hydrophobic/hydrophilic surface modification on the effectiveness of membrane cleaning. This manuscript however reports solely the preparation and performance of the more hydrophobic PES-nSMM membranes.

It is reported in the literature that the formation of membranes made by phase inversion technique depends on a number of material- and process-specific parameters including type and amount of base polymers, solvents, type and amount of additives, casting thickness, casting speed, post-treatment, conditions (temperature and composition) of the coagulation bath, and drying conditions.[17] This article investigates the impact of four key preparation factors including concentration of PES, concentration of

Correspondence to: R. M. Narbaitz (narbaitz@uottawa.ca).
Contract grant sponsors: Vietnam Government (Vietnamese Overseas Scholarship Programs-VOSP), Natural Sciences and Engineering Research Council of Canada (NSERC), Ministry of the Environment (MOE), Ontario, Canada.

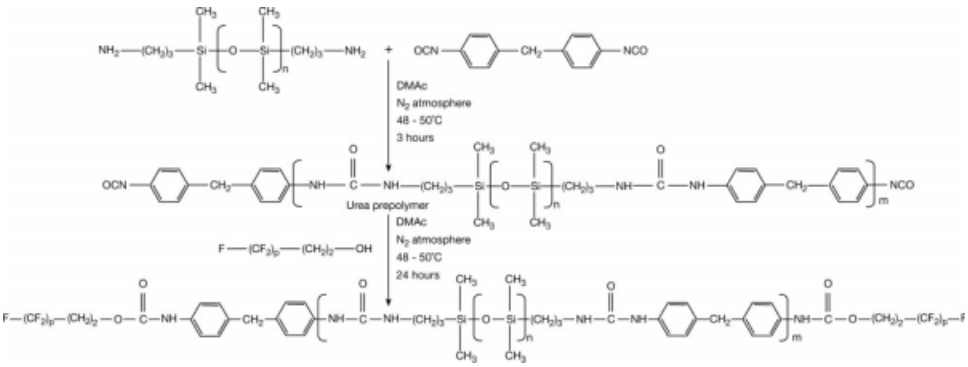

Figure 1 Schematics of nSMM synthesis.

nSMM, casting thickness, and casting speed conditions. Although the impacts would be different with different types of additives, this study incorporates a broad comparison with other research dealing with membrane modification.

EXPERIMENTAL METHODS AND ANALYSIS

Material

Poly(ether sulfone) (PES, Victrex 4100P, powder) was supplied by ICI Advanced Materials, Billingham, Cleveland, England, UK. 4,4-Methylene bis(phenyl isocyanate) (also known as diphenylmethane diisocyanate, MDI, 98%) was purchased from Sigma-Aldrich, St. Louis, MO. Oligomeric fluoroalcohol (OFA) (Zonyl fluorotelomer intermediate, 2-(perfluoroalkyl)ethanol, BA-L of average M_n 443 and 70 wt % fluorine) was supplied by Aldrich Chemical, Milwaukee, WI. The α,ω-aminopropyl poly(dimethyl siloxane) (PDMS) of average molecular weight 900 was purchased from Shin-Etsu Chemical, Tokyo, Japan. Deuterated tetrahydrofuran (THF-d8, 99.5 at% D) was purchased from CDN Isotopes, Point-Claire, PQ, Canada. Polyethylene glycol (PEG) and polyethylene oxide (PEO) (Aldrich Chemical, Milwaukee, WI) were used as probe solutes for the solute transport tests.

nSMM synthesis

The nSMM was synthesized using a two-step condensation polymerization method.[16] MDI was distilled at 150°C under 0.5 Torr. OFA and PDMS were degassed for 24 h under 0.5 mmHg. The first step was conducted in a common solvent (*N*,*N*-dimethyl acetamide, DMAc) to form polyurea prepolymer by the reaction of MDI with PDMS. Basically, 7.5 g (0.03 mol) MDI dissolved in 50 mL DMAc was mixed with 18 g (0.02 mol) PDMS in 100 mL DMAc. The prepolymer was then, in the second step, end-capped by the addition of OFA in the DMAc solvent resulting in the formation of repeated polyurethane linkages. Here, 8.86 g (0.02 mol) OFA in 50 mL DMAc was used. The MDI/PDMS/OFA molar ratio of nSMM was 3 : 2 : 2. The polymer solution was precipitated in water at room temperature and dried in an air circulation oven at 120°C for 5 days.

Figure 1 shows the steps involved in the nSMM synthesis. The chemical name of the nSMM is poly (urea-dimethylsiloxane-urethane) both ends capped by OFA. The polyurethane units are expected to anchor the nSMM to the PES that makes up the bulk of the membrane and thus minimize additive leaching.

Polymeric additive's characterizations

Fluorine and silicone content in the nSMM were measured by using an oxygen flask bomb combustion technique (Oxygen Bomb Calorimeter, Gallenkamp & Co, England). The elemental analysis of fluorine content in the nSMM was carried out using standard method in ASTM D 3761. An accurate weight (10–50 mg) of nSMM was placed into the oxygen flask bomb for combustion. After pyrohydrolysis, the fluorine (ion) was measured by an ion chromatography (Ion Chromatograph, Dionex DX1000, Sunnyvale, CA). The analysis of silicon content in the nSMM was performed by oxygen flask bomb combustion, same way as fluorine analysis, followed by acid digestion, and then analyze for silicon by inductively coupled plasma-atomic emission spectrometry (ICP-AES, Varian Liberty 110, Varian, Palo Alto, CA).

The glass transition temperature (T_g) was measured by a differential scanning calorimeter (DSC) equipped with a universal analysis 2000 program (DSC Q1000, TA Instruments, New Castle, DE). About 10 mg of polymer was put into an aluminum pan and crimped with another aluminum pan. The pans were then placed within the sample chamber of the DSC. The polymer was annealed at about 280°C for 10 min, then quenched to −50°C, and scanned at a heating rate of 10°C min^{-1}. The T_g

value was recorded at the onset point of the corresponding heat capacity transition.

The number- and weight-average molecular weight of the synthesized nSMM were measured by gel permeation chromatograph (GPC, model 410, Waters Associates, Milford, MA) equipped with a refractive index detector. Three UltraStyragel™ packed columns from Waters were placed in series. Tetrahydrofuran (THF) was used as the mobile phase at a flow rate of 0.3 mL min^{-1} at 40°C. The calibration of the GPC was performed using eight polystyrene (Shodex, Tokyo, Japan) standards with molecular weights between 1.3×10^3 and 3.15×10^6 g mol^{-1}. The standards and nSMM samples were prepared in THF (0.2 w/v% solutions), and Millenium 32 software (Waters) was used for the data acquisition.

A sample for nuclear magnetic resonance (NMR) analysis was prepared by dissolving as much polymer as possible in THF-d_8. The NMR data were collected on an AVANCE 300 NMR spectrometer (Bruker Corp., East Milton, ON). The ^{1}H-NMR spectrum was acquired under quantitative conditions with 16 scans using a 30° pulse and a 3.6 s interpulse sequence.

Preparation of membranes

Casting solutions were prepared with different concentrations of PES base polymer (14, 16, and 18 wt %) and nSMM contents (0.5, 1.5, 3.0, and 4.5 wt %) dissolved in *N*-methyl pyrrolidinone solvent. Membranes were prepared using the phase inversion method, which is commonly used for the fabrication of ultrafiltration membranes.[2] These casting dopes were cast on a glass plate with a predetermined thickness (0.2 or 0.25 mm) at different casting speeds (1.5 cm s^{-1}-fast and 0.25 cm s^{-1}-slow). The different film thicknesses were obtained by using casting bars with different gaps between the casting part of the bar and the glass plate. The casting speed referred to the speed at which the casting bar was moved from one end of the glass plate to the other to create a flat sheet film that has an area of roughly 165 cm^2. The cast films were then immediately immersed into the gelation media (water, 4°C) where they hardened. The membrane preparation variables, whose impact was assessed, were PES concentration, nSMM concentration, thickness of the cast solution film, and the casting speed. Table I shows the membrane code and the corresponding variables.

TABLE I
Description of Membranes

Membrane code	PES (wt %)	nSMM (wt %)	Thickness (mm)	Casting speed (cm s^{-1})
M1	18	4.5	0.20	0.25
M2	18	4.5	0.20	1.5
M3	18	4.5	0.25	0.25
M4	18	4.5	0.25	1.50
M5	16	4.5	0.20	1.50
M6	14	4.5	0.20	1.50
M7	18	3.0	0.20	0.25
M8	18	3.0	0.20	1.50
M9	18	1.5	0.20	0.25
M10	18	1.5	0.20	1.50
M11	18	1.5	0.25	0.25
M12	18	1.5	0.25	1.50
M13	18	0.5	0.20	1.50
M14	18	0.5	0.25	1.50
M15	18	0.0	0.20	1.50

Membrane analysis and testing

The contact angle of membrane surfaces was measured using VCA Optima goniometer (AST Products, Billerica, MA). Water content was determined by gravimetric analysis.[18] Morphological examination of the top surface was made using scanning electron microscopy (SEM, model JSM-6400, Japan Electron Optics Limited, Japan). The pore size and the pore size distribution were determined by the solute transport method.[19] Fourier transform infrared (FTIR) spectroscopy was also used to observe the presence of functional groups in the membrane. The FTIR spectrometer (Varian 1000, Scimitar series, Varian, Palo Alto, CA) was equipped with diamond w/ZnSe lens single reflection attenuated total reflection (ATR) plate. An IR source at 45° incident angle was used. Samples of both the top and bottom membranes surfaces were mounted for IR analysis. The spectra were measured in the transmittance mode over a wave number range of 4000–600 cm^{-1} at a resolution of 4 cm^{-1}.

All membrane tests followed the testing protocol described in details by Dang et al.[19] and were performed using a six-crossflow cell-in-series system described by Mosqueda-Jimenez et al.[13] Briefly, membranes were precompacted for 1 h at 552 kPa (80 psig) and room temperature. This was followed by 50 h of pure water permeation (PWP) monitoring (i.e., ultra-pure water filtration at 345 kPa (50 psig), at flowrate of 1.1 Lpm and room temperature), then followed by the PEG/PEO solute transport quantification, and completed by a 50-h long filtration/fouling test using Ottawa River water (ORW) (at the same feed flow rate and pressure). The solute transport method is based on ultrafiltration experiments with solutes of different known molecular weights (i.e., PEG with molecular weights of 6, 10, 20, 35, and 100 kDa). An assumption is made that PEG/PEO are probe solutes that do not interact with membrane pores. Hence, the solute separation is assumed to be solely by sieving mechanism. All filtration tests were conducted in duplicate.

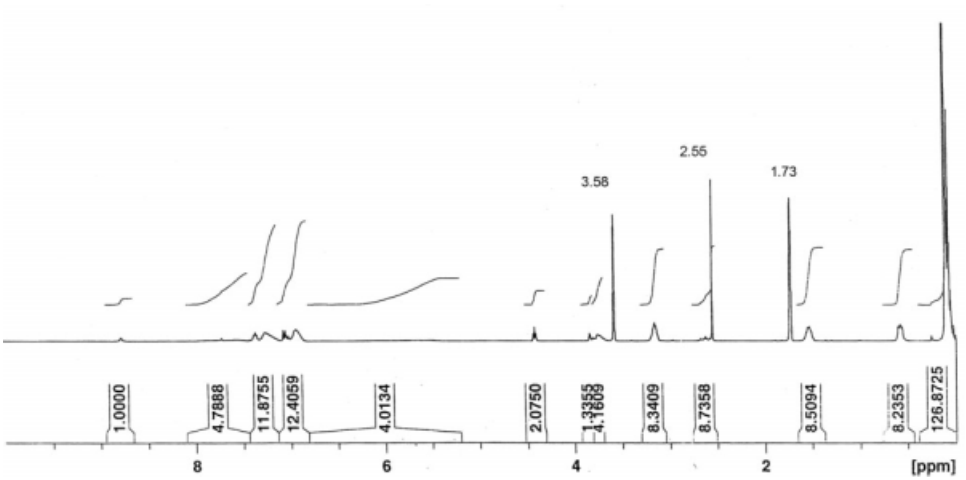

Figure 2 NMR spectrum of nSMM.

RESULTS AND DISCUSSION

Polymer analysis

The fluorine and silicone content in the nSMM are 11.75 and 11.52 wt %, respectively. The values of number-average molecular weight (M_n) and weight-average molecular weight (M_w) of the nSMM are 12.8 and 27.1 kDa, respectively. The glass transition temperature (T_g) of the nSMM is above 280°C. The T_g of PES is 221.4°C. The *n*, *m*, and *p* are the numbers of repeat units of siloxane, prepolymer polyurea, and difluoromethane within nSMM respectively (Fig. 1). The value of subscript "*p*" is 7.58, which was calculated from the molecular weight of OFA. The value of "*n*" calculated from the average molecular weight of PDMS is 9.81. Based on the stoichiometry of the synthesis and number-average molecular weight of polymer, "*m*" has been calculated, which is 10.14 for nSMM. These values were calculated based on the assumption that all the reactants were consumed. The characteristic peaks of the ^{1}H-NMR are displayed in Figure 2 and summarized in Table II.

TABLE II
The Assignments of ^{1}H-NMR Characteristic Peaks of nSMM

Assignment	ppm
CH_3 (PDMS)	0.11
CH_2 (PDMS) adjacent to the Si bond	0.58
CH_2 (PDMS) middle of *n*-propyl group	1.53
CH_2 (OFA) adjacent to the CF_2 bond	2.62
CH_2 (PDMS) adjacent to the urea bond	3.16
CH_2 between the phenyl groups of MDI	3.68–3.76
CH_2 (OFA) adjacent to the urethane bond	4.42
Urea NH	5.80, 7.72
Aromatic hydrogen (MDI)	6.94–7.39
Urethane NH	8.78

3.58 and 1.73 ppm peaks are due to THF-d_8 (C_4D_8O); 2.55 ppm peak is due to the solvent DMAc.

The functional groups listed in Table II were corresponding to the peaks in Figure 2 going from right to left. Those characteristic peaks confirm the types of linkages within the nSMM.

FTIR analysis

The presence of functional groups at the surfaces of the asymmetric membrane was examined by FTIR-ATR spectroscopy. The FTIR spectra of both top and bottom surfaces of the membranes with and without nSMM are shown in Figure 3(a). The spectrum of the base PES membrane shows the peaks at 1571 and 1486 cm^{-1}, which are for aromatic bands. The sharp adsorption peaks at 1323 and 1151 cm^{-1} are attributed to the asymmetric and symmetric stretching vibration of sulfone (O=S=O) group. The sharp adsorption peak at 1241 cm^{-1} is due to stretching vibration of ether (Ar—O—Ar) linkage. The top and bottom surface of PES membrane without nSMM are the same [Fig. 3(aA, aB)], whereas for the PES-nSMM membranes the peak intensity at the top surface [Fig. 3(aC)] is much higher than the bottom surface [Fig. 3(aD)]. As for the membrane in which nSMM is blended the broad peak appeared at $\sim$ 3331 cm^{-1} due to the N—H stretching. Peaks [Fig. 3(a, spectrum C)] appeared at 2961, 1645, 1258, 1085, 1020, and 796 cm^{-1}, which can be corresponded to C—H (CH_3 and CH_2 vibration) stretching, C—O (urea and urethane) stretching, Si—CH_3 (δ stretching), CF_2 stretching, Si—O—Si stretching, and Si—CH_3 (γ stretching) of nSMM, respectively. However, the clear indication of N—H stretching, C—H stretching, Si—CH_3 (γ and δ stretching), Si—O—Si stretching, etc., demonstrated that the bottom surface also contained nSMM [Fig. 3(a spectrum D)]. The FTIR subtract spectra (top surface minus bottom

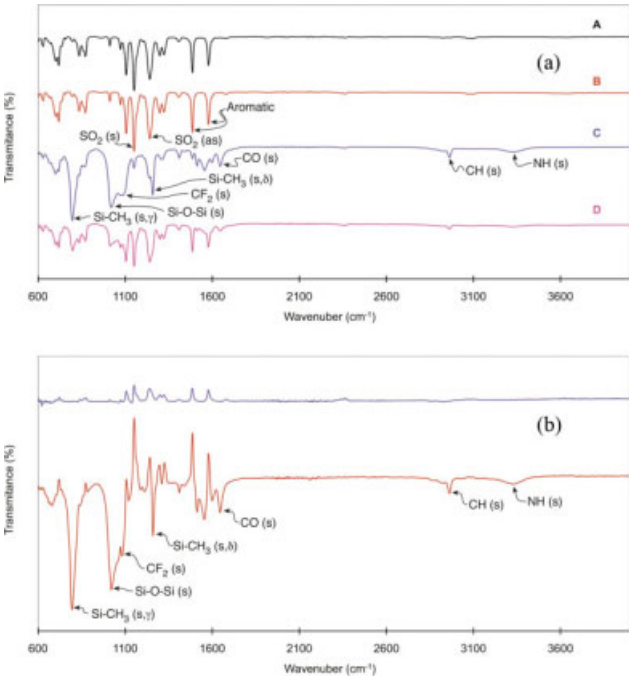

Figure 3 a: FTIR spectra of (A) top surface of PES membrane without nSMM, (B) bottom surface of PES membrane without nSMM, (C) top surface of PES membrane with 4.5% nSMM, and (D) bottom surface of PES membrane with 4.5% nSMM. b: FTIR subtract spectra consist of (A) top surface minus bottom surface of PES membrane and (B) top surface minus bottom surface of PES membrane with 4.5 wt % nSMM. [Color figure can be viewed in the online issue, which is available at www.interscience.wiley.com.]

surface) are shown in Figure 3(b) for the membranes without and with nSMM. As expected, peaks are very small for the PES membrane without nSMM, whereas much larger peaks were obtained from the PES membrane with nSMM. These results confirm the migration of nSMM to the top surface.

SEM of different modified nSMM membranes

As nSMM migrates quite fast to the surface because of its high hydrophobicity, it alters significantly the surface chemistry and morphology of membranes.[20] Figure 4 presents the SEM images (5000× magnification) of 13 membrane top surface samples evaluated (refer to Table I for their compositions). SEM images of membranes 7 and 8 are not sharp so they are not included in the figure. Compared with the control PES membranes (M15), the nSMM membranes seem to have rougher surfaces. This shows evidence of nSMM migration to the modified membrane surfaces. Nevertheless, the changes in additive concentrations, PES concentrations, and casting speeds did not have a clear impact on the apparent membrane roughness.

It is worth noting that when we added more nSMM, the casting solutions became less viscous (i.e., viscosity of 3 wt % nSMM + 18 wt % PES is 622 cP, whereas for the 4.5 wt % nSMM + 18 wt % PES, viscosity is 573 cP). This is probably due to the reduction in chain entanglement of the host polymer (PES), which occurs when a sufficiently large amount of nSMM is added to the polymer solution. Compared with the control PES solution (viscosity of 410 cP), blending nSMM additive made the solution more viscous. The membrane surfaces are not as shiny or smooth as the control PES membranes M15 (Fig. 4) but rough and dry with colonies of small mounds, possibly from polymer aggregations that were evident, even with the smallest amounts of nSMM added (0.5 or 1.0 wt %) as observed on the surfaces of membranes M13 and M14 (Fig. 4). The surfaces are however very hydrophobic with a contact angle of 91°, whereas that of the control PES (M15) is about 70°. Increasing the evaporation time prior to gelation can result in contact angles of more than 120°.[21] It is interesting that higher percentage of nSMM does not guarantee more hydrophobic nature, as confirmed in several previous studies.[13,22,23]

Key factors controlling hydrophobic membrane modification

Impacts of four main factors including base polymer concentration, nSMM concentration, thickness of the cast film, and the casting speed on the membrane characteristics and performance were evaluated.

Effect of polymer concentration

Figure 5 reveals the correlation between volume throughput (cumulative permeate) and dissolved organic carbon (DOC) rejection over 50-h filtration test for different PES concentrations (nSMM concentration was kept consistently at 4.5 wt %). Note that the natural organic matter (NOM) in ORW was quantified in term of DOC and ORW with a DOC of 6.8 mg L^{-1} was used as a feed in the filtration test. Membranes M2 (18 wt % of PES) exhibited quite low permeate flux, whereas membrane M6 (14 wt % of PES) yielded highest volume throughput. As a trade-off, M6 had quite low DOC removal (maximum about 30%). Membrane M5 with 16 wt % PES compensates for the lower fluxes by having volume throughput and high DOC removal (initially close to 90%). It seems that adding more base polymer delayed the demixing process, leading to less porous membranes with lower water production.[24,25]

When the membranes were subjected to visual inspection after the filtration experiments, deposition of NOM was observed in a very limited area leaving most of the membrane surface without

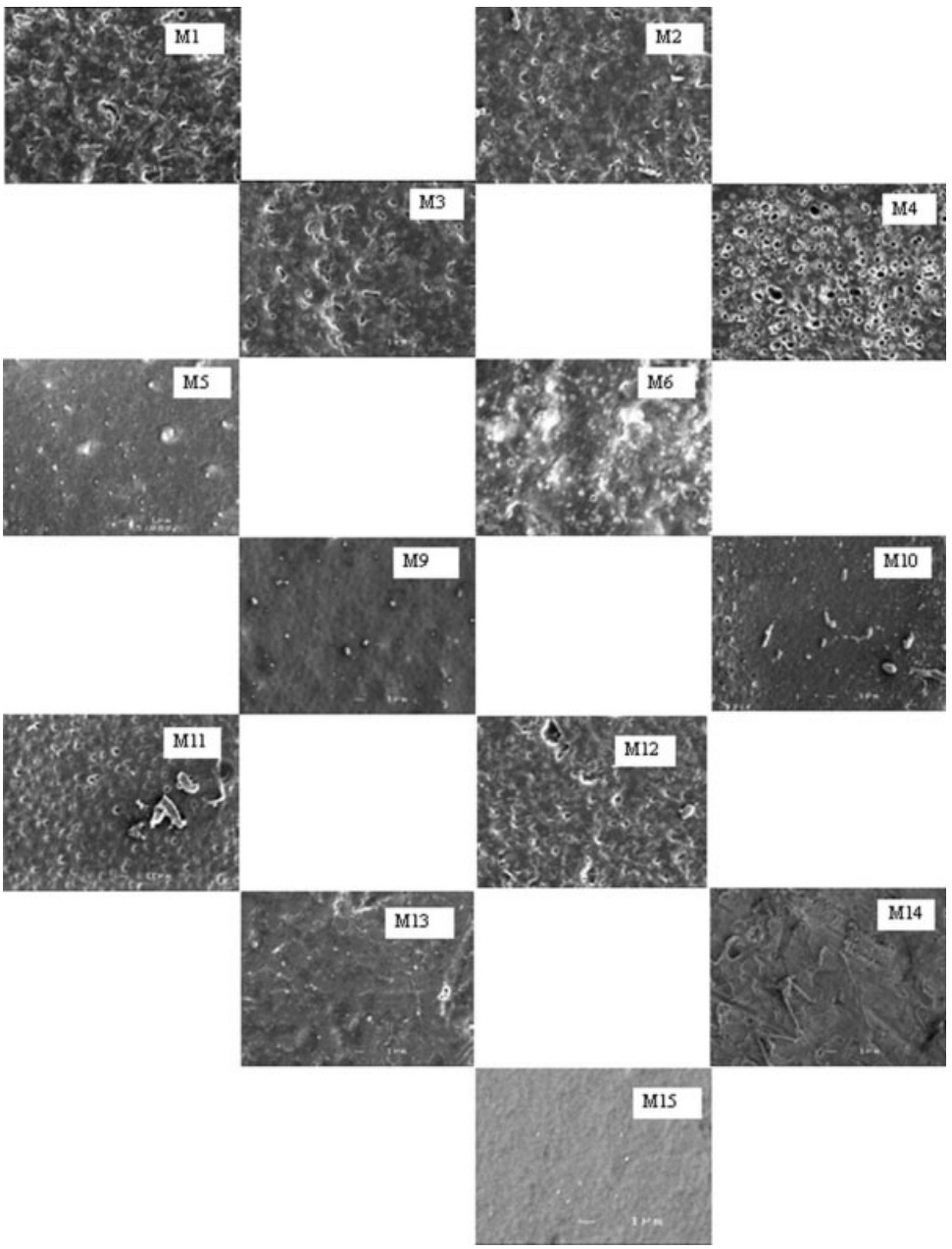

Figure 4 SEM of membranes with different nSMM contents (For membrane codes, refer Table I).

contamination. This means that instead of depositing on the membrane surface, most of NOMs went into the pores, some trapped inside the pores, and some were transported through the pores under the hydraulic pressure.

Figure 6 shows surface free energy (correlated to contact angles and tabulated using SE-2500 software, which accompanies the VCA Optima goniometer) and water content for the above three membranes (M2, M5, and M6). No significant difference was observed. This was consistent with an earlier observation[23] that the contact angle did not statistically change with the change in the host PEI (polyetherimide) concentration. However, higher base polymer content in the casting solution led to an increase in the mechanical strength of that membrane.[26]

Effect of additive concentration

When the PES concentration was fixed at 18 wt %, homogeneous casting solutions could not be obtained even by vigorous mixing for nSMM concentrations of more than 5%. At the nSMM concentration of 1%, the solution looked homogeneous in the beginning, but phase separation took place after a few hours. This is consistent with the earlier study where the phase separation was observed at the nSMM concentration of 2%.[22] However, casting the

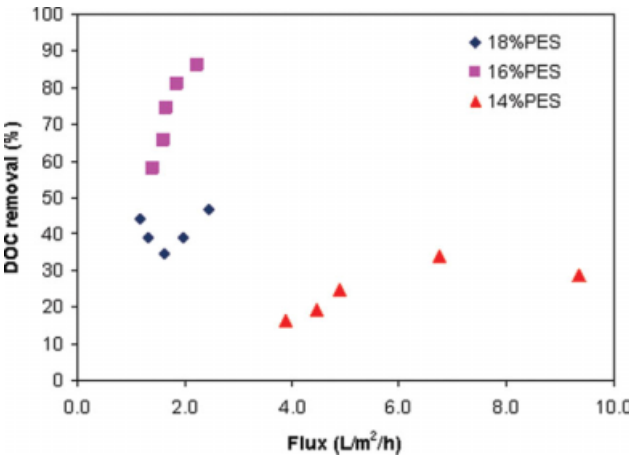

Figure 5 Flux and DOC correlation. Membranes: M2 (18 wt % PES), M5 (16 wt % PES), and M6 (14 wt % PES); nSMM concentration, 4.5 wt %; cast film thickness, 0.2 mm; casting speed, 1.5 cm s^{-1}. [Color figure can be viewed in the online issue, which is available at www.interscience.wiley.com.]

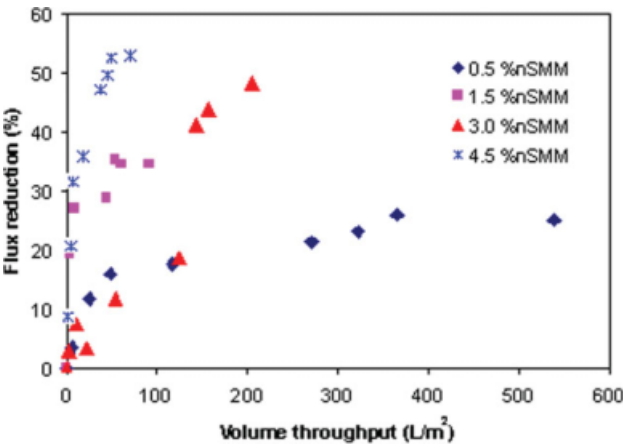

Figure 7 Flux reduction versus time. Membranes: M2 (4.5% nSMM), M8 (3.0% nSMM), M10 (1.5% nSMM), and M13 (0.5% nSMM); PES concentration, 18%; film thickness, 0.2 mm; casting speed, 1.5 cm s^{-1}. [Color figure can be viewed in the online issue, which is available at www.interscience.wiley.com.]

polymeric solution was still possible after remixing if the nSMM concentration was below 5%. Likewise, a high percentage of nSMM did not guarantee more hydrophobic membrane, that is, the contact angles were statistically the same with the increasing nSMM dosage, even though their contact angles were always higher than those of the control PES membrane by 15°–20°.

Figure 7 shows flux reduction versus volume throughput (cumulative permeate) for the membranes prepared from the casting solutions with different amounts of nSMM. Flux reduction was determined by following equation:

$$\text{Flux reduction } (\%) = \frac{J_{wi} - J_{wf}}{J_{wi}} \times 100, \qquad (1)$$

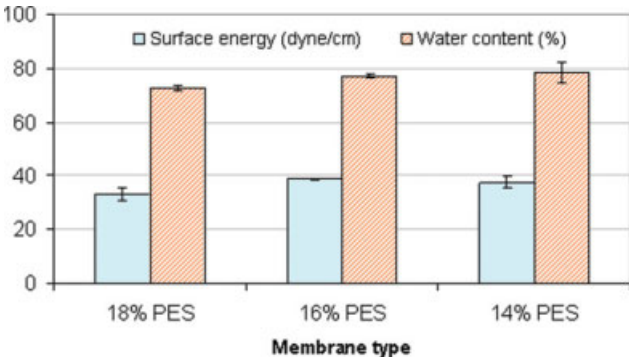

Figure 6 Surface energy and water content. Membranes: M2 (18 wt % PES), M5 (16 wt % PES), and M6 (14 wt % PES); nSMM concentration, 4.5 wt %; cast film thickness, 0.2 mm; casting speed, 1.5 cm s^{-1}. [Color figure can be viewed in the online issue, which is available at www.interscience.wiley.com.]

where J_{wi} is the initial flux during the fouling test with ORW (L m^{-2} h^{-1}) and J_{wf} is the final flux during the fouling test with ORW (L m^{-2} h^{-1}).

It is obvious that the flux reduction increases with the increasing dose of nSMM. Membrane M2 with 4.5 wt % nSMM had lowest cumulative water production and highest flux resistance. It is understandable because the additive is hydrophobic. For this reason the membrane with 0.5 wt % nSMM was chosen as the best dose in manufacturing this type of membranes for the future membrane cleaning study.

Another parameter for quantifying fouling is the fouling resistance, R_f. It is calculated based on the fluxes for clean water and the fouling solution using the following equations:

$$J_{wo} = \frac{\Delta P}{\mu \times R_m}. \qquad (2)$$

$$J_{wf} = \frac{\Delta P}{\mu \times (R_m + R_f)}, \qquad (3)$$

where J_{wo} and J_{wf} (L m^{-2} h^{-1}) are the flux after 50-h filtration with pure water (Milli-Q water) and final flux after 50-h filtration with NOM-containing water (ORW), respectively. R_m and R_f (L m^{-1}) are membrane resistance and fouling resistance parameter, respectively. μ (Ns m^{-2}) is the fluid viscosity and ΔP (N m^{-2}) is transmembrane pressure difference.

Based on Figure 8, membrane M13 (0.5% nSMM) has the smallest fouling resistance and membrane M2 (4.5% nSMM) the largest. Through visual inspection after opening the test cells, it was found that membrane M13 (0.5% nSMM) had the largest degree of NOM deposition, which made the membrane surface look slightly brown. On the other hand, the

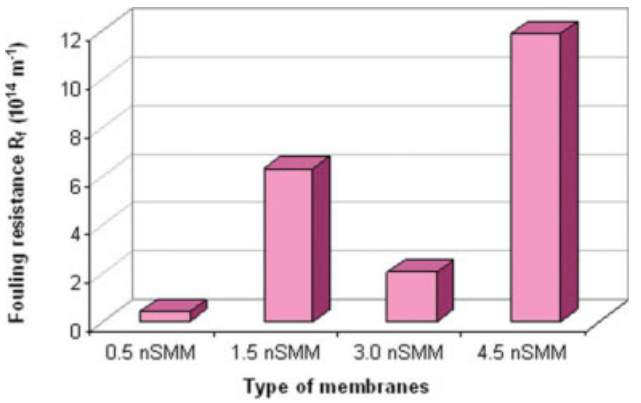

Figure 8 Fouling resistance after 50 h of filtration. Membranes: M2 (4.5 wt % nSMM), M8 (3.0 wt % nSMM), M10 (1.5 wt % nSMM), and M13 (0.5% nSMM); PES concentration, 18%; film thickness, 0.2 mm; casting speed, 1.5 cm s^{-1}. [Color figure can be viewed in the online issue, which is available at www.interscience.wiley.com.]

surfaces of membrane M2 (4.5% nSMM) and M10 (1.5% nSMM) remained clean and white. Another observation was that the DOC removals by membranes M8 (3.0% nSMM) and M13 (0.5% nSMM) were lower than that of M2 (4.5% nSMM).

One interesting conclusion could be drawn here is that with the exception of 3.0 wt % nSMM, the more nSMM is added, the higher fouling resistance is and the lower DOC removal achieved (data not shown). The deviation of the membranes with 3 wt % nSMM from the normal trend is probably ascribed to the abnormal pore characteristics of this particular membrane and/or the distribution of hydrophobic fraction of the NOM used in the experiment with this particular membrane. The higher cake resistance with increasing nSMM concentration might be due to the interaction between the hydrophobic chains (i.e., fluoro-hydrocarbon chains) on the membrane surface and the hydrophobic fraction in NOM.[18] Charge repulsion cannot be the cause of this phenomenon because NOM is normally negatively charged while the surface of PES-nSMM membranes (containing fluoro-hydrocarbon chains on the surface) should be neutral or even positive. If that was the case, higher nSMM concentration (assumingly more neutral) would attract NOM better. Nevertheless, the lowest nSMM concentration (0.5 wt %) membrane attracted more NOM on and through membranes, proving via its lowest fouling resistance.

Effect of casting speed

The PWP flux and the initial DOC rejection (after 15 min) at two casting speeds of 0.25 (slow) and 1.5 cm s^{-1} (fast) were presented in Figure 9. Three nSMM concentrations (1.5, 3.0, and 4.5 wt %) in the casting solutions were used. For each nSMM concentration, both PWP and initial DOC rejection increased as the casting speed was increased. This result is consistent with the study of Sharpe et al.[27] using polysulfone hollow fiber membranes for gas separation. They found that the asymmetric membranes made under high shear rates tended to exhibit higher pressure-normalized flux and selectivity. They have attributed this to the greater molecular orientation in the skin layer. In our study, higher casting speed was proportional to the higher shear rate, leading to greater molecular orientation and leaving bigger gaps (pores) between two aligned macromolecular nodules. When the casting speed or shear rate was not strong, the alignment of nodules was less and the gaps (pores) were smaller, resulting in smaller pores or lower MWCO. The casting speed had no effects on the apparent roughness of membranes (See M1 versus M2, M3 versus M4, etc., in Fig. 4).

Effect of membrane thickness

Figure 10 shows molecular weight cutoff (MWCO, molecular weight that yields 90% solute separation) and mean pore size data for two different thicknesses of the cast films. Two nSMM concentrations in the casting solutions were investigated. The data reveal that both MWCO and the mean pore size decreased as the thickness increased. The effect of film thickness has been reported by several researchers.[26,28,29] Suk et al.[26] rendered that reduced membrane thickness would lower the surface energy with higher content of fluorine. Contact angles increased from 80° to 106° for the thinnest membranes. In this study, the same trend was observed, that is, contact angles increased slightly from 89.8° ±

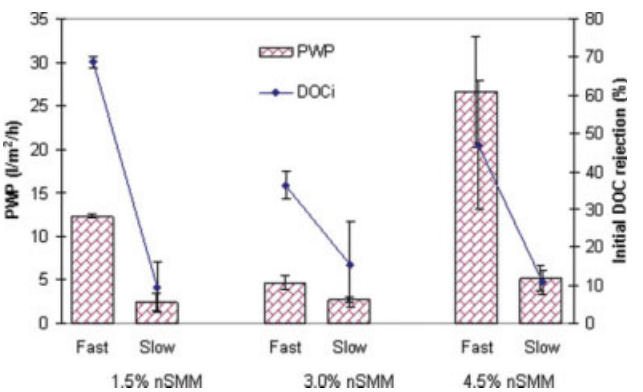

Figure 9 PWP and initial DOC rejection. Membranes: M10 (1.5 cm s^{-1}, 1.5% nSMM), M9 (0.25 cm s^{-1}, 1.5% nSMM), M8 (1.5 cm s^{-1}, 3.0% nSMM), M7 (0.25 cm s^{-1}, 3.0% nSMM), M2 (1.5 cm s^{-1}, 4.5% nSMM), and M1 (0.25 cm s^{-1}, 4.5% nSMM); PES concentration, 18%; cast film thickness, 0.2 mm. [Color figure can be viewed in the online issue, which is available at www.interscience.wiley.com.]

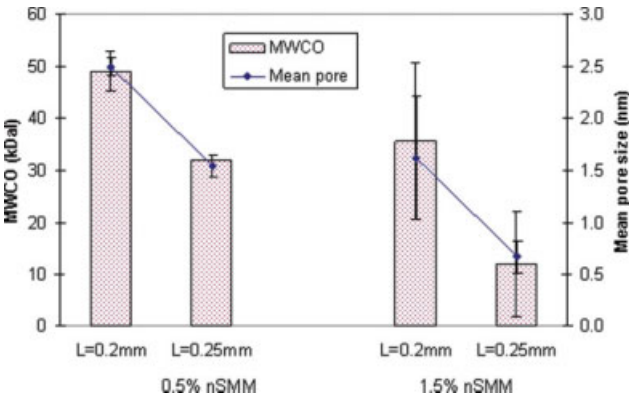

Figure 10 Pore characteristics. Membranes: M13 (0.2-mm thickness, 0.5% nSMM), M14 (0.25-mm thickness, 0.5% nSMM), M10 (0.2-mm thickness, 1.5% nSMM), and M12 (0.25-mm thickness, 1.5% nSMM); PES concentration, 18%; casting speed, 1.5 mm. [Color figure can be viewed in the online issue, which is available at www.interscience.wiley.com.]

1.7° for M14 to 91.6° ± 1.0° for M13 and from 80.6° ± 3.5° for M12 to 87.1° ± 0.1° for M10. In Veerapur's study,[28] they found that increase in the membrane thickness resulted in a decrease in flux with a somewhat lesser profound effect on the selectivity of the membranes in their pervaporation study. It is noted that the Veerapur's study was for hydrophilic membranes. Although the same phenomenon has been reported in the literature, no proper elucidation has been presented. In our case, the explanation again lies on the shear stress during the film casting. As the shear stress is directly proportional to casting velocity and inversely proportional to film thickness (shear stress = (viscosity)* (velocity/thickness)), the shear stress increases by either increasing the casting velocity or by decreasing the thickness. Therefore, decreasing the thickness has the same effect on shear stress as increasing the casting speed. As discussed in the effect of casting speed, the increased shear stress presumably led to the larger pore size as a result of the better alignment of the polymer nodules. Thus, the thinner membrane films had a larger mean pore size or MWCO.

To test if the effects of the four variables involved in the membrane casting are statistically significant, an one-way analysis of variance (ANOVA) test was conducted using Minitab 15 statistical software (Minitab, State College, PA). The null hypothesis (H_0), in which the effect of any particular independent variable on each of the response variables does not exist, was rejected if P-value ≤ 0.05 ($\alpha = 0.05$ or 5%). Therefore, for the P-values to be statistically significant they should be ≤ 0.05. Table III summarizes the results of the statistical analysis. Apparently, only additive concentration had significant impacts on the DOC removal, flux reduction, and final flux. It is worth noting that these changes in performance because of different additive concentrations were not accompanied by statistically significant changes in contact angles.

Fouling Modeling

This section is concerned with the fouling mechanism for membranes of different nSMM loading. To study the mechanisms leading to membrane fouling, the common practice consists of assuming that one of the four fouling mechanisms (e.g., cake formation, intermediate blocking, pore constriction (standard blocking), and complete blocking) takes place. The differential rate laws corresponding to all possible fouling mechanisms were proposed by Hermia[30] for dead-end filtration under constant applied pressure:

$$\frac{dJ}{dt} = kJ(J)^{2-n}, \tag{4}$$

where k is a fouling coefficient and n is a dimensionless filtration constant, which depends on the type of filtration. The constant n has values of 0, 1, 1.5, and 2 for cake filtration, intermediate blocking, standard blocking, and complete blocking, respectively.

The filtration experiments in this study however used cross-flow mode. Cross-flow mode has been claimed to enhance mass transfer processes that induce back transport from the membrane surface, leading to lower net flux of foulant to the membrane surface.[31] The unifying equation for cross-flow filtration applied in this study was as follows:

$$\frac{dJ}{dt} = -k(J - J*)(J)^{2-n}, \tag{5}$$

where J^* is a critical flux (L m^{-2} h^{-1}) and n has the same values as in eq. (4).

Determination of k and J^* with corresponding n was performed using MATLAB 7.0 (Math Works, Natick, MA).

TABLE III
***P*-Values of the Independent Variables Obtained from the Analysis of Variance (One-Way ANOVA) for the Performance Variables**

	P-values		
Source of variation	Solute rejection	Flux reduction	Final Flux
PES concentration (wt %)	0.07—No	0.744—No	0.207—No
nSMM concentration (wt %)	0.014—Yes	0.004—Yes	0.041—Yes
Casting speed (m s^{-1})	0.167—No	0.385—No	0.097—No
Thickness of membrane film (mm)	0.684—No	0.400—No	0.091—No

TABLE IV
Fitting Parameters and Mean Square Residual (MSR) for Membranes of Different nSMM Loading

n (dimensionless)	k (dimensionless)	J^* (L m^{-2} h^{-1})	MSR
M13 (0.5 wt % of nSMM)			
0.0	0.0003	6.3364	1.0663
1.0	−0.0211	10.5017	0.5231
1.5	−0.0185	10.6172	0.9807
2.0	−0.2672	10.5195	0.5843
M10 (1.5 wt % of nSMM)			
0.0	0.2957	1.6436	0.4681
1.0	0.0045	3.4272	0.6870
1.5	−0.0612	1.5849	0.3584
2.0	−0.5279	1.7952	0.0515
M8 (3.0 wt % of nSMM)			
0.0	0.0052	2.8620	2.0494
1.0	−0.0067	2.1613	1.9776
1.5	−0.0566	2.4426	2.8842
2.0	−0.0157	0.0952	1.3758
M2 (4.5 wt % of nSMM)			
0.0	0.1062	1.2006	0.0114
1.0	−0.0838	1.2260	0.0067
1.5	−0.1141	1.3028	0.0089
2.0	−0.1632	1.2480	0.0089

Table IV presents the regressed model coefficients as well as mean square residuals (MSRs). Figure 11 shows the experimental data (circles) and simulations (lines) for different fouling mechanisms (n values) for a representative membrane (M2, which has 4.5% nSMM). In this particular case, three different mechanisms appear to describe the data quite well. However, the best fitting (i.e., has the lowest MSR) mechanism varies for every single case. Increasing concentration of nSMM presumably affected the fouling mechanism as the best fitting model changed. Intermediate blocking ($n = 1$) best described the fouling of 0.5 wt % nSMM membranes, whereas complete blocking ($n = 2$) was the main fouling mechanisms for 1.5 and 3.0% nSMM membranes, while for the 4.5 wt % nSMM membranes, the MRS values are too close to distinguish among the various mechanisms. (Fig. 11).

It is to be noted that the MWCOs of 3.0 and 4.5 wt % PES-nSMM membranes were from 3.5 to 5 kDa with mean pore sizes of less than 0.5 nm. Loose NF membranes often have MWCOs ranging from less than 1 kDa to several kDa for the treatment of drinking water.[32] Therefore, they can be considered as loose nanofiltration (NF) membranes, for which the major fouling mechanism was found to be intermediate or complete blocking.[33]

Mosqueda-Jimenez et al.[15] found in their study that cake formation was the best fitted model, which was definitely not the case for this study. The difference may be ascribed to different membranes and testing protocols even though a similar feed (NOM containing water) was used. It is worth noting that the values of J^*, the critical flux, were close to the final fluxes after 50-h testing period. In addition, when the degree of fouling became more serious (from $n = 0$ to 2), the fluxes often decreased more slowly and k showed larger negative values. In other words, smaller values of k represent less dramatic flux decline. It was consistent with several studies.[18,30]

The single mechanism modeling in some cases does not fit well the experimental data due to the possible fact that more than one mechanism affecting membrane fouling. A combined cake formation and pore constriction model developed by Kilduff et al.[31] for cross-flow filtration mode was therefore introduced.

The area of open pores was expressed as follows:

$$A_{\text{open}} = A_T \exp\left[-\alpha C_b t\left(\frac{\Delta P}{\mu R_m} - J*\right)\right], \qquad (6)$$

where A_T ($=A_{\text{open}} + A_{\text{blocked}}$) is the nominal membrane area (m^2), A_{open} the area of unblocked or open pores (m^2), A_{blocked} the area of membrane blocked by foulant (m^2), α the pore blockage parameter (m^2 kg^{-1}), C_b the bulk concentration of the solute (kg m^{-3}), ΔP the applied pressure (Pa), μ the solution viscosity (kg m^{-1} s^{-1}), and R_m is the membrane resistance (m^{-1}).

The rate of cake resistance, which is assumed to be equal to the mass of solute transported to the surface, was integrated analytically from $R_{c,0}$ to R_c:

$$\frac{dR_c}{dt} = \alpha_c(A_T - A_{\text{open}})C_b\left(\frac{\Delta P}{\mu(R_m + R_c)} - J*\right), \qquad (7)$$

where α_c is the specific resistance of the cake (m^{-1} kg^{-1}) and $R_{c,0}$ is the resistance of the initial deposit (m^{-1}).

Finally, the modeled flux was calculated with the equation:

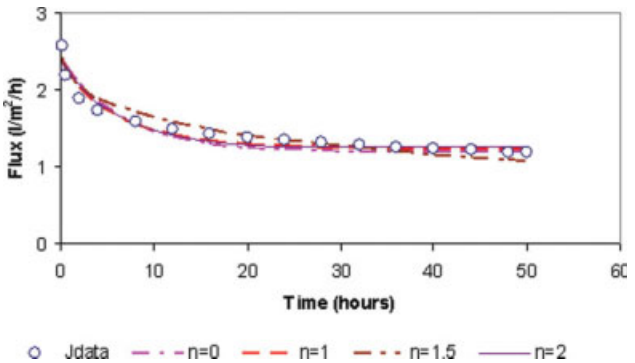

Figure 11 Fitting of experimental data (open circle) by different n values for M2 (4.5 wt % nSMM) membranes. [Color figure can be viewed in the online issue, which is available at www.interscience.wiley.com.]

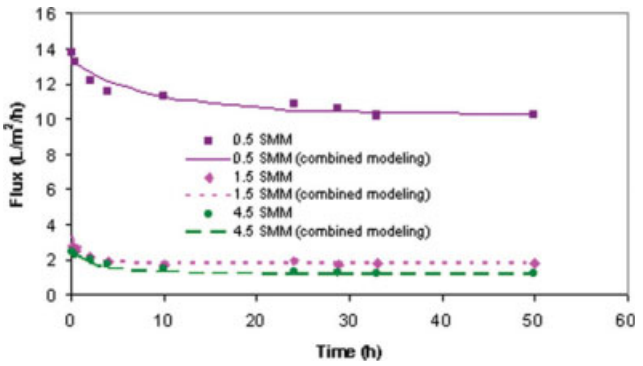

Figure 12 Flux reduction with time for combined-mechanism model for different types of membranes.

$$J_T = \frac{A_{\text{open}}\Delta P}{\mu R_m} + \frac{(A_T - A_{\text{open}})\Delta P}{\mu(R_m + R_c)}, \quad (8)$$

Parameters such as α, α_c, R_c, and J^* were optimized using Microsoft Excel Solver and MATLAB 7.0 (Math Works, Natick, MA). Mosqueda-Jimenez et al.[15] found that the combined mechanism fitted the experimental data better than the single one with a smaller mean square error. It is confirmed again by this study (Fig. 12 and Table V).

The MSRs of combined-mechanism model are all smaller than those of single-mechanism model (Table V), proving the combined simulates better the fouling mechanism. Autopsy of fouled membranes suggested that the irreversible fouling layer was initially formed by pore blocking of small particles followed by strong interaction of fouling layer with mainly dissolved materials and by fouling layer compaction due to permeation drag.[34]

Again, for the case of the 3.0% SMM membranes, as the data were not smooth, the simulated flux did not fit well. Its MSR was small because the values of fluxes were small, so the difference was not significant. Regardless of the case of 3.0% SMM membranes, the specific cake resistance parameter α_c, pore block parameter α, and the resistance of the initial fouling layer $R_{c,0}$ seem to be slightly affected with the increasing concentration of SMM. Moreover, the higher the flux permeation was, the lower was the resistance. This agrees with the fact that higher SMM concentration membranes had very little NOM deposition on the surface at the end of the experiment (membranes were almost clean).

CONCLUSIONS

Several conclusions can be drawn from observing the results of this study as follows:

1. The synthesis of nSMM was successful. Characterization of nSMM was performed by NMR, GPC, DSC, and elemental analysis. FTIR results confirmed the enrichment of nSMM at the top surface through migration during the cast process.
2. Among the four affecting factors studied in this research (polymer concentration, additive concentration, casting speed, and membrane thickness), only the additive concentration impacted the membrane performance (i.e., DOC removal and flux reduction) to a statistically significant level. This was confirmed by one-way ANOVA statistical analysis. Even though other factors such as membrane thickness may alter the pore characteristic, their effect on membrane performance was marginal.
3. Single fouling mechanism modeling suggested that the fouling by NOM of these hydrophobic membranes behaved like loose NF membranes, which involved in mostly intermediate or complete pore blocking. A combined cake formation and pore constriction model however simulated better the fouling mechanism for those membranes.
4. During the filtration with NOM-containing river water, most of NOM penetrated through the membrane to the permeate side probably because of the morphology of PES-nSMM membranes. They were rougher with deeper and bigger features, which were more likely to deform under pressure.

NOMENCLATURE

$J_{\text{pure water}}$	flux of pure water (L m^{-2} h^{-1})
$J_{\text{fouled water}}$	flux of fouled water (L m^{-2} h^{-1})
M_n	number-average molecular weight
M_w	weight-average molecular weight

TABLE V
Fitting parameters for combined fouling mechanism model

Membranes	α	α_c	$R_{c,0}$	J*	MSR	MSR (Single)[+]
0.5 SMM	0.3020	1.05E+20	1.01E+17	10.255	0.011	0.523
1.5 SMM	0.3885	1.50E+22	3.89E+17	1.795	0.006	0.052
3.0 SMM	0.1885	1.50E+19	3.69E+17	2.690	0.202	1.376
4.5 SMM	0.5619	1.50E+22	5.05E+17	1.182	0.001	0.007

[+]The smallest MSR obtained from single model.

T_g	glass transition temperature (°C)
R_c	fouling resistance (m^{-1})
R_m	resistance of membrane (m^{-1})
$R_{c,0}$	resistance of the initial deposit (m^{-1})
A_{open}	area of unblocked or open pores (m^2)
$A_{blocked}$	area of membrane blocked by foulant (m^2)
C_b	bulk concentration of the solute (kg m^{-3})

Greek letters

ΔP	trans-membrane pressure (Pa)
μ	fluid viscosity (kg m^{-1} s^{-1})
Δp	threshold value of pressure (Pa),
σ	surface tension of the feed solution (mJ m^{-2})
r	pore radius (mm)
α	pore blockage parameter (m^2 kg^{-1})
α_c	specific resistance of the cake (m^{-1} kg^{-1})

References

1. Kesting, R. E. Synthetic Polymeric Membranes; McGraw-Hill Book Company: New York, NY, 1971.
2. Matsuura, T. Synthetic Membranes and Membrane Separation Processes; CRC Press: Boca Raton, FL, 1994.
3. Pinnau, I.; Freeman, B. D. In Membrane Formation and Modification (ACS Symposium Series 744); Pinnau, I., Freeman, B. D., Eds.; American Chemical Society: Washington, DC, 2000; p 1.
4. Lafrenière, L.Y.; Talbot, F. D. F.; Matsuura, T.; Sourirajan, S. Ind Eng Chem Res 1987, 26, 2385.
5. Bowen, W. R.; Doneva, T. A.; Yin, H. B. J Membr Sci 2001, 181, 253.
6. Lokhare, H. R.; Kumbharkar, S. C.; Bhole, Y. S.; Kharul, U. K. J Appl Polym Sci 2005, 101, 4378.
7. Idris, A.; Zain, N. M.; Noordin, M. Y. Desalination 2007, 207, 324.
8. Arthannareeswaran, G.; Mohan, D.; Raajenthiren, M. Appl Surf Sci 2007, 253, 8705.
9. Wang, J.; Xu, Y.; Zhu, L.; Li, J.; Zhu, B. Polymer 2008, 49, 3256.
10. Rahimpour, A.; Madaeni, S. S.; Mehdipour-Ataei, S. J Membr Sci 2008, 311, 349.
11. Rahimpour, A.; Madaeni, S. S.; Taheri, A. H.; Mansourpanah, Y. J Membr Sci 2008, 313, 158.
12. Su, Y.; Li, C.; Zhao, W.; Shi, Q.; Wang, H.; Jiang, Z.; Zhu, S. J Membr Sci 2008, 322, 171.
13. Mosqueda-Jimenez, D. B.; Narbaitz, R. M.; Matsuura, T. Sep Purif Technol 2004, 37, 51.
14. Mosqueda-Jimenez, D. B.; Narbaitz, R. M.; Matsuura, T.; Chowdhury, G.; Pleizier, G.; Santerre, J. P. J Membr Sci 2004, 231, 209.
15. Mosqueda-Jimenez, D. B.; Narbaitz, R. M.; Matsuura, T. J Appl Polym Sci 2006, 99, 2978.
16. Suk, D. E.; Matsuura, T.; Park, H. B.; Lee, Y. M. J Membr Sci 2006, 277, 177.
17. Mulder, M. Basic Principles of Membrane Technology; Kluwer Academic Publishers: Dordrecht, The Netherlands, 1996.
18. Dang, H. T.; Amelot, C.; Rana, D.; Narbaitz, R. M.; Matsuura, T. J Appl Polym Sci 2010 (to appear).
19. Dang, H. T.; Narbaitz, R. M.; Matsuura, T. J Membr Sci 2008, 323, 45.
20. Khayet, M.; Suk, D. E.; Narbaitz, R. M.; Santerre, J. P.; Matsuura, T. J Appl Polym Sci 2003, 89, 2902.
21. Zhang, L.; Chowdhury, G.; Feng, C.; Matsuura, T.; Narbaitz, R. M. J Appl Polym Sci 2003, 88, 3132.
22. Pham, V. A.; Santerre, J. P.; Matsuura, T.; Narbaitz, R. M. J Appl Polym Sci 1999, 73, 1363.
23. Khayet, M.; Feng, C. Y.; Matsuura, T. J Membr Sci 2003, 213, 159.
24. Peng, N.; Chung, T. S.; Wang, K. Y. J Membr Sci 2008, 318, 363.
25. Cabasso, I.; Klein, E.; Smith, J. K. J Appl Polym Sci 1977, 21, 165.
26. Suk, D. E.; Chowdhury, G.; Matsuura, T.; Narbaitz, R. M.; Santerre, P.; Pleizier, G.; Deslandes, Y. Macromolecules 2002, 35, 3017.
27. Sharpe, I. D.; Ismail, A. F.; Shilton, S. J. Sep Purif Technol 1999, 17, 101.
28. Veerapur, R. S.; Gudasi, K. B.; Aminabhavi, T. M. J Membr Sci 2007, 304, 102.
29. Li, D. F.; Chung, T. S.; Ren, J. Z.; Wang, R. Ind Eng Chem Res 2004, 43, 1553.
30. Hermia, J. J Trans Inst Chem Eng 1982, 60, 183.
31. Kilduff, J. E.; Mattaraj, S.; Sensibaugh, J.; Pieracci, J. P.; Yuan, Y.; Belfort, G. Environ Eng Sci 2002, 19, 477.
32. Wan, L.-S.; Xu, Z.-K.; Huang, X.-J.; Che, A.-F.; Wang, Z.-G. J Membr Sci 2006, 277, 157.
33. Jung, B.; Yoon, J. K.; Kim, B.; Rhee, H.-W. J Membr Sci 2004, 243, 45.
34. Choi, H.; Zhang, K.; Dionysiou, D. D.; Oerther, D. B.; Sorial, G. A. Sep Purif Technol 2005, 45, 68.